J. Mol. Biol. (1996) **261**, 62–71

JMB

Towards a Molecular Understanding of the Elasticity of Titin

Wolfgang A. Linke[1]*, Marc Ivemeyer[1], Nicoletta Olivieri[2] Bernhard Kolmerer[2], J. Caspar Rüegg[1] and Siegfried Labeit[2]

[1]*Institute of Physiology II University of Heidelberg Im Neuenheimer Feld 326 D-69120 Heidelberg Germany*

[2]*European Molecular Biology Laboratory, Meyerhofstrasse 1 D-69012 Heidelberg Germany*

**Corresponding author*

Vertebrate striated muscle behaves elastically when stretched and this property is thought to reside primarily within the giant filamentous protein, titin (connectin). The elastic portion of titin comprises two distinct structural motifs, immunoglobulin (Ig) domains and the PEVK titin, which is a novel motif family rich in proline, glutamate, valine and lysine residues. The respective contributions of the titin Ig and the PEVK sequences to the elastic properties of the molecule have been unknown so far. We have measured both the passive tension in single, isolated myofibrils from cardiac and skeletal muscle and the stretch-induced translational movement of I-band titin antibody epitopes following immunofluorescent labelling of sites adjacent to the PEVK and Ig domain regions. We found that with myofibril stretch, I-band titin does not extend homogeneously. The Ig domain region lengthened predominantly during small stretch, but such lengthening did not result in measurable passive tension and might be explained by straightening, rather than by unfolding, of the Ig repeats. At moderate to extreme stretch, the main extensible region was found to be the PEVK segment whose unravelling was correlated with a steady passive tension increase. In turn, PEVK domain transition from a linearly extended to a folded state appears to be principally responsible for the elasticity of muscle fibers. Thus, the length of the PEVK sequence may determine the tissue-specificity of muscle stiffness, whereas the expression of different Ig domain motif lengths may set the characteristic slack sarcomere length of a muscle type.

Keywords: titin or connectin; muscle elasticity; PEVK domain; passive tension; myofibril mechanics

Introduction

Titin, also referred to as connectin, is a polypeptide of extremely high molecular mass (Maruyama *et al*., 1977; Wang *et al*., 1979), which spans each half of the sarcomere from the Z-disc to the M-line (Fürst *et al*., 1988). Within the A-band segment, titin is bound along the thick filament and is therefore stiff under physiological conditions, whereas the I-band section is extensible (Fürst *et al*., 1988; Itoh *et al*., 1988; Whiting *et al*., 1989; Trombitas *et al*., 1991). The extension properties of the titin filament in the I-band might explain a principal feature of striated muscle, its elasticity, i.e. the capability of relaxed muscle fibers to ''passively'' retract following a stretch. Over the last decade, there has been increasing evidence that the titin filament is indeed the element mainly responsible for the elasticity of both cardiac and skeletal muscle (Magid & Law, 1985; Horowits *et al*., 1986; Funatsu *et al*., 1993; Granzier & Wang, 1993; Maruyama, 1994; Trinick, 1994). However, the molecular mechanism as to how the titin filament supports sarcomere elasticity has remained obscure.

Initial concepts on titin filament elasticity assumed that the extension properties of immunoglobulin (Ig) and fibronectin-type III (FN3) repeats, which make up 90% of titin's mass (Labeit & Kolmerer, 1995), may represent the molecular basis of this elasticity. Both repeat types fold into globular domains composed of seven strands of antiparallel β-sheets (Holden *et al*., 1992; Leahy *et al*., 1992; Pfuhl & Pastore, 1995; Politou *et al*., 1995). It was proposed that during stretch, the Ig and FN3 titin domains may unfold, which might

† Abbreviations used: SL, sarcomere length; MIR, main immunogenic region.

0022–2836/96/310062–10 $18.00/0

account for the generation of passive tension (Soteriou *et al*., 1993; Erickson, 1994). Furthermore, since the A-band section of titin also consists of Ig and FN3 domains (Labeit *et al*., 1990), it was suggested that at higher forces, A-band titin domains might be recruited to contribute to elasticity (Wang *et al*., 1993). An alternative hypothesis to explain titin filament elasticity has recently been put forth, and proposes that the interdomain linker sequences between the I-band titin domains might be extensible. During stretch of these ''hinge'' regions, the exposure of hydrophobic residues to water may be relevant for the onset of passive tension (Politou *et al*., 1995). In short, the hypotheses proposed as yet have assumed that rapid and reversible conformational transitions within the Ig and FN3 domains may represent the molecular basis of titin elasticity.

Another structural motif type, apart from the Ig and FN3 repeats, was recently found within the I-band titin portion and was referred to as the PEVK segment, because proline, glutamate, valine and lysine residues constitute ~70% of its sequence (Labeit & Kolmerer, 1995). The PEVK titin was suggested to be relevant for muscle elasticity, because it is expressed in different length versions in cardiac, psoas and soleus muscles, which differ remarkably in their passive tension properties. However, not only has the PEVK segment varying length in different muscle tissues, but also another I-band titin segment, composed solely of tandemly arranged Ig repeats (poly-Ig titin), is expressed in different lengths in these three muscle types (Labeit & Kolmerer, 1995). The differential expression of both the PEVK and the poly-Ig titin segments, in correlation with tissue stiffness, thus warrants to identify the relative contribution of the two distinct I-band titin segments to passive tension as a first step towards a molecular understanding of titin's elasticity. Therefore, we have characterized the elastic properties of both the tandem Ig domain and the PEVK region by a combination of immunofluorescence microscopic techniques and single myofibril mechanics (Linke *et al*., 1993, 1994). The results of this study demonstrate that the main extension of I-band titin during myofibril stretch occurs within the region containing the PEVK sequences. Moreover, extension of the PEVK region requires considerable force and is readily reversible. This suggests that conformational transitions within the PEVK motif family likely represent the molecular basis of sarcomere elasticity. A summary of this work has already been published in abstract form (Linke *et al*., 1996a).

Results

Titin is expressed in different isoforms in various muscle tissues (Wang *et al*., 1991; Horowits, 1992), with both I-band motif classes, the tandem Ig and PEVK titin segments, being expressed in different length versions (Labeit & Kolmerer, 1995). Therefore, we chose to investigate three types of muscle expressing a long (soleus), intermediate (psoas), and short (cardiac) isoform of known tandem Ig and PEVK titin content. An overview of the I-band titin arrangement in cardiac and soleus muscle is shown schematically in Figure 1. We measured

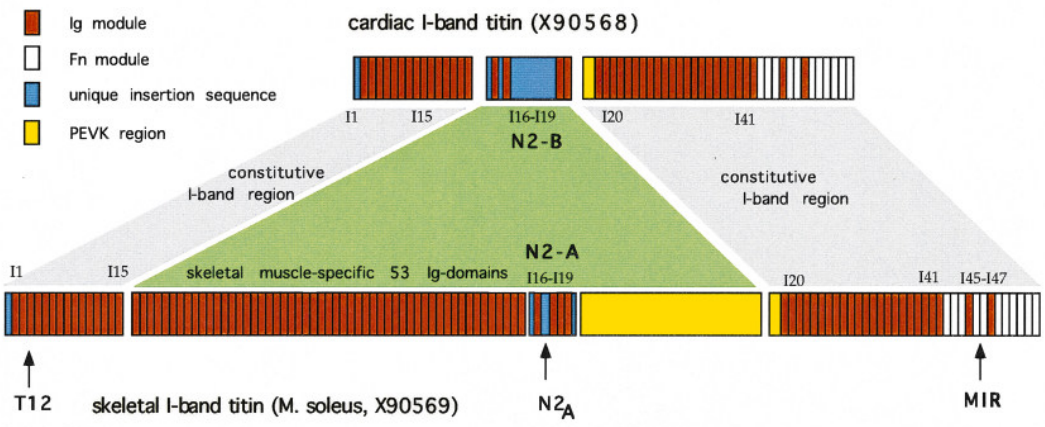

Figure 1. Overview of the primary structure of cardiac and soleus I-band titin. Schematically shown is a comparison of the structure of sequenced titins from human soleus and human heart. The EMBL data library accession numbers are noted as well. The area marked in green refers to the differentially spliced sequences: soleus titin has a fourfold longer N-terminal tandem Ig segment and a 13-fold longer PEVK domain, compared with cardiac titin. Although not shown in the Figure, also cardiac muscle expresses an isoform containing the N2-A titin segment. The epitope positions of three of the antibodies used in this study are indicated (T12, $N2_A$ = N2-A, MIR). The T12 antibody assigns to the domains I2 to I4, near the N-terminal end of the first tandem Ig segment (Sebestyen *et al*., 1995; Labeit & Kolmerer, 1995). The MIR (main immunogenic region of titin) comprises the domains I45 to I47 (Gautel *et al*., 1993). For the N2-A segment, a polyclonal antibody was raised against the unique sequence insertion indicated, which is specific to the N2-A splice variant. Sequence analysis has shown that in rabbit, the I-band titin domain architecture of soleus and cardiac muscle is similar to that of the respective human muscle types. Rabbit psoas muscle expresses an isoform where both the N-terminal tandem Ig segment and the PEVK titin region are intermediate in length, compared with the respective segments of the cardiac and soleus isoforms (unpublished results).

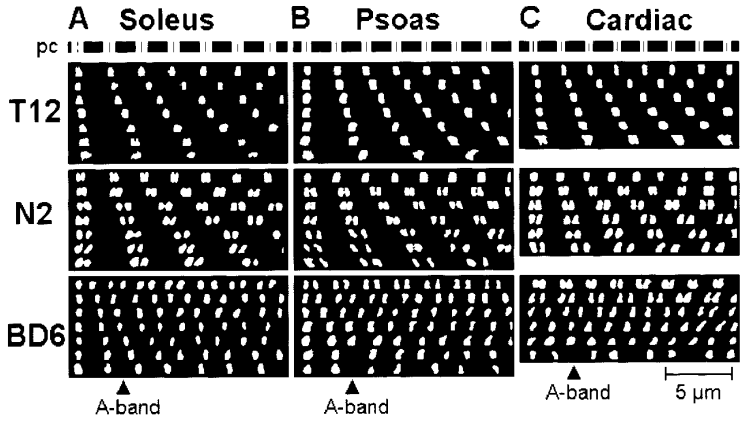

Figure 2. Representative fluorescence images of antibody-labelled myofibrils. After labelling with one of the antibodies (T12, N2-A, BD6) and the fluorophore, myofibrils were stretched to a series of SLs. A, Soleus myofibrils to 2.4, 2.7, 3.0, 3.3, 3.6, ~4.0, and ~4.4 μm; B, psoas myofibrils to 2.2, 2.5, 2.8, 3.1, 3.4, ~3.8, and ~4.2 μm; C, cardiac myofibrils to 1.9, 2.2, 2.5, 2.8, ~3.1, and ~3.4 μm (from top to bottom, respectively). The average slack SL of soleus myofibrils was (±SD) 2.26 (±0.11) μm (n = 15), whereas in psoas and cardiac myofibrils, it was 2.09 (±0.10) μm (n = 14) and 1.87 (±0.09) μm (n = 23), respectively. In extremely stretched myofibrils near the strain limit, SL inhomogeneity was increased, so that only approximate SL values could be given. To accommodate the SL inhomogeneities, we measured the lengths of individual sarcomeres, and correlated it with the titin antibody spacing within these sarcomeres. pc = scheme of striation image of myofibrils in the phase-contrast microscope, with the black zones representing the A-bands and the white zones the I-bands (including the Z-disc).

both the passive tension response of single, isolated myofibrils to stretch, using a sensitive force transducer (Fearn *et al*., 1993; Linke *et al*., 1993), and the extensibility of different I-band titin regions by immunofluorescence microscopy. It was considered advantageous to perform immunofluorescence measurements under the light microscope, for this enabled us to study dynamic aspects of titin domain extension on chemically non-fixed preparations. All data shown below were obtained from rat muscle but preliminary experiments with rabbit muscle gave similar results.

Differential mobilities of I-band titin epitopes upon myofibril stretch

In both cardiac and skeletal muscle, the tandem Ig and the PEVK titin segments are separated by a distinct linker sequence, which has been suggested to localize within the N2-line region (Labeit & Kolmerer, 1995). However, since the correspondence of this linker sequence with the sarcomere's N2-line has not been conclusively shown, we will in the following refer to it as the (putative) N2-titin segment. Two types of linker sequences are known and have been termed N2-A and N2-B, because they are specific to the splice pathways N2-A and N2-B, respectively (Labeit & Kolmerer, 1995). To monitor the epitope position of the N2-titin segments within the half-sarcomere, we raised specific antibodies against both the N2-A and the N2-B sequence. When single myofibrils were exposed to N2-A-specific antibodies and a fluorophore-marked secondary antibody, we found avid staining within minutes of exposure, in cardiac, psoas and soleus muscle preparations. In contrast, the N2-B antibody stained exclusively cardiac myofibrils (data not shown), indicating that the N2-B-titin isoform is specific to cardiac muscle. This also showed that, at the level of a single cardiac myofibril, the N2-A and N2-B isoforms are co-expressed.

N2-A-labelled myofibrils from the three muscle types were stretched to a series of sarcomere lengths (SLs), and the translational movement of the antibody epitopes was monitored in the fluorescence microscope (see Materials and Methods). We then compared the extent of epitope movement with that found with two other, epitope-mapped, monoclonal antibodies, T12 and BD6, which label sites flanking the elastic I-band titin portion. T12 binds to titin at the N1-line (Fürst *et al*., 1988), ~100 nm from the center of the Z-disc, whereas BD6 stains titin near the A/I junction (Whiting *et al*., 1989), ~40 nm from the end of the thick filament inside the A-band.

The T12 antibody labelled two closely spaced stripes, one in each half-sarcomere near the Z-disc, in all three muscle types investigated. Frequently, those two stripes were observed as a single, broad labelling site (Figure 2, top panels, Figure 3, lowest curves). Upon stretch, the antibody position remained stationary relative to the Z-disc. Only with extreme extensions did the epitope-epitope distance (across the Z-disc) increase slightly, and labelling became fuzzy. These results are consistent with earlier electron microscopic findings in both skeletal and cardiac muscle, which showed that with physiological stretch, the Z-disc-N1-line region is inextensible (Trombitas & Pollack, 1993; Trombitas *et al*., 1995).

With the N2-titin antibody, a different pattern of translational movement was found for each muscle type. In soleus myofibrils, the antibody spacing across the Z-disc was approximately 0.3 μm at slack SL, but increased to ~0.7 μm upon stretch to an SL of 2.8 μm (Figure 2A, middle panel; Figure 3A, middle curve). Above this length, and up to extreme SLs above 4 μm (strain limit), however, the slope of the N2-titin spacing curve was greatly reduced. In psoas myofibrils, stretch from slack SL

to 2.5 to 2.6 μm resulted in a steady increase in antibody spacing from ~0.25 to ~0.5 μm (Figure 2B, middle panel; Figure 3B, middle curve). Above 2.6 μm SL, the epitope–epitope distance remained almost unchanged up to SLs slightly longer than 3 μm, where it began to markedly increase again. The maximum spacing was reached at the strain limit SL of ~3.6 μm. In cardiac myofibrils held at slack SL, the N2-titin antibody epitopes were usually so closely spaced that they appeared as one single, broad stripe. Only above 2 μm SL was the epitope–epitope distance sufficiently large to become clearly detectable (Figure 2C, middle panel; Figure 3C, middle curve). With further stretch, the labelled sites continued to move apart, until at SLs near 3 μm (strain limit), epitope labelling became fuzzy, probably indicating a destruction of the regular titin filament alignment.

When BD6-labelled myofibrils were stretched, the epitope-epitope distance across the Z-disc increased and corresponded closely to changes in SL, for extensions over the entire physiological range and in all three muscle types investigated (Figure 2, lowest panels; Figure 3, top curves). This regular pattern of translational movement abruptly changed at SLs near the strain limit, where previously bound A-band titin was suddenly released into the I-band, thereby increasing the A-band titin length dramatically (arrowheads in Figure 2). However, release of A-band titin, also referred to as ''yielding'' (Wang *et al*., 1993), was never observed during extensions within the physiological SL range. Interestingly, myofibrils from different muscle types yielded at different SLs: soleus near 4 μm, psoas at ~3.6 μm, and cardiac muscle at 3.3 to 3.4 μm. Because yielding was observed in both freshly prepared and glycerinated myofibrils, we assumed that the phenomenon was genuine.

Differences in titin epitope extension patterns suggest differential extension of tandem Ig and PEVK titins

To confirm the characteristic extension behavior of the N2-titin epitope, we compared it with that of two other, previously published, I-band titin antibodies, 9D10 and MIR. The latter is present in the blood sera of myasthenia gravis (with thymoma) patients and comprises the domains I45 to I47 (Gautel *et al*., 1993; cf. also Figure 1); it probably labels just inside the I-band near the A/I junction (Aarli *et al*., 1990). 9D10 has not been epitope mapped yet, but has been shown to label titin within the central segment of its elastic I-band portion (Wang & Greaser, 1985).

With both the 9D10 and the MIR antibodies, we found that sarcomere stretch resulted in a continuous increase in epitope spacing, measured across the Z-disc (Figure 4A to C). The slope of the MIR epitope spacing curve was steeper than that of the 9D10 curve, as expected from the sarcomeric positions of the antibody epitopes. The MIR epitope remained stationary relative to the M-line, confirming that the I-band titin region near the A/I junction is stiff during physiological extensions. Only above the strain limit SL could the A-band titin yielding phenomenon be observed again, in all three muscle types investigated (cf. above). As for the 9D10 antibody, the slope of the epitope spacing curve at short SLs was comparable with that found for the initial section of the N2-titin curve in both soleus and psoas myofibrils. However, for these small stretches, the 9D10 curve was shifted leftward by 0.1 to 0.2 μm, compared with that of the N2-titin curve, indicating that the 9D10 antibody must bind C-terminally from the N2-titin segment. Above SLs of ~2.8 μm (soleus) or ~2.6 μm (psoas), the epitope spacing continued to increase steadily, in contrast to that of the N2-titin antibody. Interestingly, at

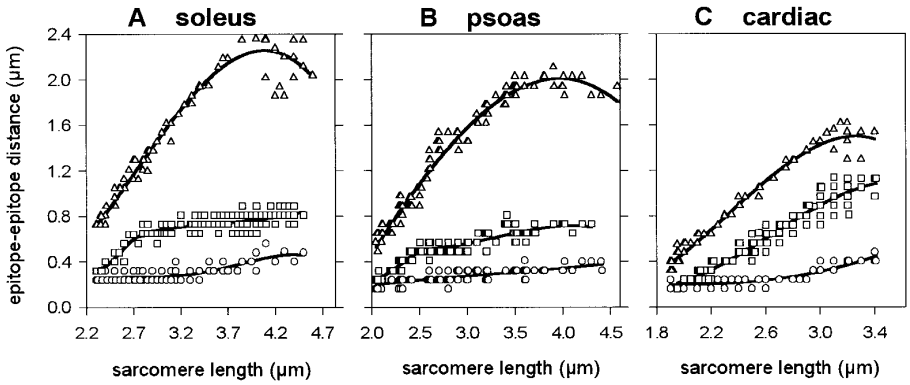

Figure 3. Summary of results of fluorescence measurements, using the BD6, N2-A and T12 antibodies. Data points from all experiments were summarized for each muscle type in plots of SL *versus* epitope–epitope distance (across the Z-disc). The number of myofibrils investigated was 6 to 15 per antibody and muscle type. All curves were obtained by third order regression of the pooled data points. Since the T12 epitopes and, in psoas and cardiac myofibrils, the N2-titin epitopes at slack SL frequently appeared as one broad stripe within the Z-disc region (cf. Figure 2), we plotted stripe width in such cases, rather than epitope–epitope distance. Symbols: △, BD6; □, N2-antibody; ○, T12.

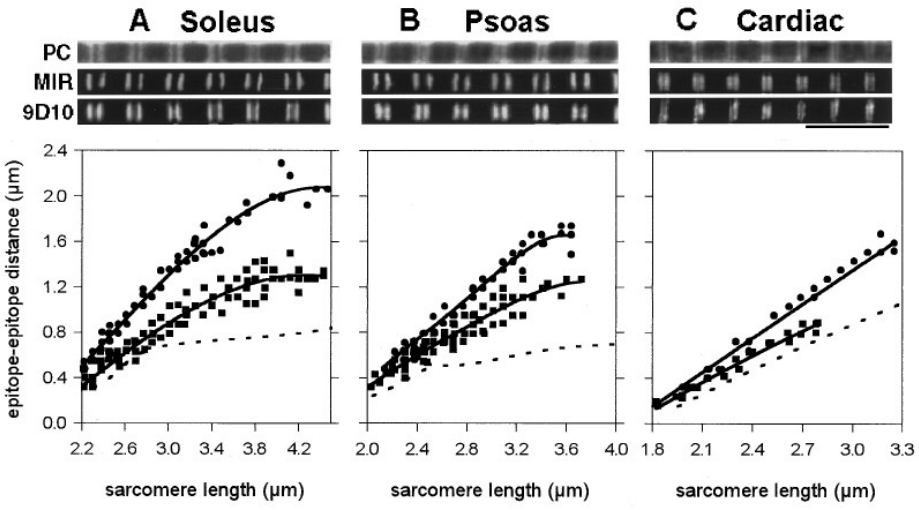

Figure 4. Results of immunofluorescence measurements, using the MIR and 9D10 antibodies. Top panels show typical phase-contrast (PC) and fluorescence images of the three myofibril types used. Before labelling with the titin antibodies, both soleus and psoas myofibrils were stretched to SL = 2.4 μm, cardiac myofibrils to SL = 2.1 μm. Graphs below show pooled data from all fluorescence measurements, using the MIR and 9D10 antibodies. Epitope–epitope distance was measured across the Z-disc. The number of myofibrils investigated was five to nine per antibody and muscle type. Continuous curves were fitted by third order regressions. The broken lines represent the regression curves for the N2-A titin antibody data, taken from Figure 3. Symbols: ●, MIR; ■, 9D10. The scale bar represents 5 μm.

least in the skeletal myofibrils, the 9D10 epitope width increased noticeably at SLs above 3 μm (data not shown). In cardiac myofibrils, on the other hand, the slope of the 9D10 epitope spacing curve was similar to that of the N2-titin curve, over the entire SL range investigated. It was also comparable with that measured in rat cardiac cells by Granzier *et al*. (1996), who used immuno-electron microscopic methods. As in the skeletal myofibrils, we observed an ∼0.1 μm leftward shift of the 9D10 curve, relative to the N2-titin curve, while epitope widening was not apparent. Altogether, the 9D10 data suggest that this antibody binds closer to the A/I junction than the N2-titin antibody, possibly within the PEVK region. Thus, it is reasonable to conclude that the differences in extension behavior between the 9D10 and the N2-titin antibodies may result from the differential extensibility of the tandem Ig and PEVK titins.

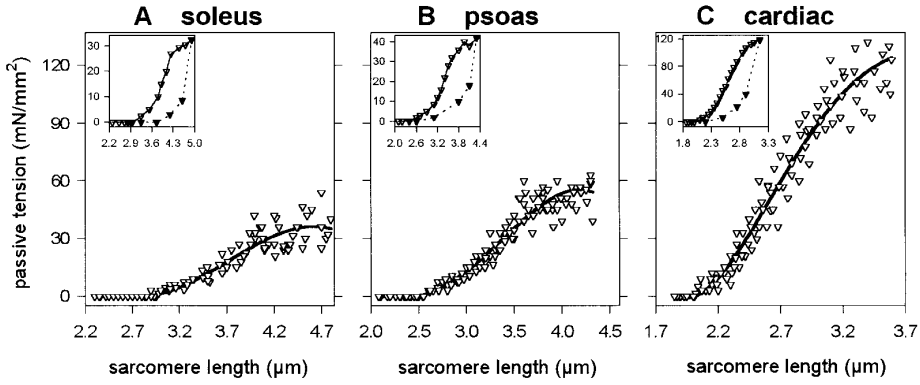

Figure 5. Summary of results of passive tension measurements. Passive force was measured in four to nine rat myofibrils per tissue type. Curves were obtained by third order regression of the pooled data points. The shape and magnitude of the rat psoas and cardiac passive tension curves are comparable with those previously measured in single rabbit psoas and cardiac myofibrils (Bartoo *et al*., 1993; Linke *et al*., 1994), indicating that the mechanical properties of the titin filaments in the respective muscle types appear to be similar in the two species. This also argues for a similar I-band titin architecture of tandem Ig domains and PEVK sequences in these two species. Insets: passive tension recordings from a typical, single experiment for each myofibril type. Shown are stretch-release cycles, with the continuous lines representing stretch data and the broken lines release data. In all three muscle types, we observed a strain limit at extremely stretched myofibril lengths, as indicated by a flattening of the passive tension-SL curves. After extreme stretch to beyond the strain limit length, myofibrillar slack SL was generally increased. Large hysteresis is apparent as well, but was much smaller when myofibrils were stretched to moderate SLs only. A more comprehensive documentation of stretch-release cycles on single cardiac myofibrils can be found elsewhere (Linke *et al*., 1996b).

Tandem Ig and PEVK titin segments differ in their contribution to passive tension

To investigate the contribution of both the Ig domain and the PEVK region to passive tension, we measured the force response of relaxed single myofibrils to stretch (Figure 5). The onset of a significant passive tension rise occurred at quite different SLs in the three types of muscle preparations. In soleus myofibrils, which exhibited an average slack SL of ~2.25 μm, passive tension became detectable at SLs of ~2.9 μm (A). In psoas (B, slack SL, ~2.1 μm) and cardiac (C, slack SL, ~1.85 μm) myofibrils, passive tension could be detected at much shorter SLs of ~2.6 and ~2.1 μm, respectively. Similarly, passive tension in larger preparations from the respective muscle types begins to increase at comparable SLs (Salviati *et al*., 1990; Horowits, 1992; Granzier & Irving, 1995). Remarkably, at least in the skeletal muscle preparations, passive tension thus becomes apparent SLs only at those at which the tandem Ig segment (T12-N2) has almost ceased to extend (cf. Figure 3A and B).

With further sarcomere extension, passive tension increased steadily. At extremely stretched SLs, myofibrils reached a strain limit, as indicated by a flattening of the passive tension-SL curves (Figure 5). Such flattening usually began at SLs of ~4.2 (soleus), ~3.6 (psoas), and ~3.0 (cardiac) μm and thus, corresponded closely with the observed ''yield point'' SLs (cf. Figure 3) and with the strain limit SLs reported previously for both skeletal (Wang *et al*., 1993; Granzier & Wang, 1993) and cardiac muscle (Granzier & Irving, 1995). At the strain limit SL, the passive tension magnitude was approximately two times higher in cardiac, compared with skeletal, myofibrils, which hints at the possibility that cardiac titin is potentially able to bear higher stresses than skeletal titins (Linke *et al*., 1996b). However, within the physiological SL range (maximum SLs, much greater than 3 μm in skeletal muscle, but only ~2.4 μm in the heart; Allen & Kentish, 1985; Rodriguez *et al*., 1992), the tension magnitude was similar in all three muscle types. Finally, when tension after small to moderate stretch was released, myofibrils were able to fully retract to their initial slack SL, indicating titin's elastic nature (cf. Linke *et al*., 1994). Only after an extreme stretch was the slack SL of a myofibril increased irreversibly (Figure 5, insets).

Discussion

In this study, we have characterized the elastic properties of different isoforms of titin in single skeletal and cardiac myofibrils. The use of single myofibrils for mechanical studies on titin is advantageous in that these preparations lack any extramyofibrillar structures, which in larger specimens, such as myocytes, may contribute to passive tension; the passive mechanical properties of a myofibril should thus reliably reflect those of a single titin strand (cf. Linke *et al*., 1994). And the myofibril preparation has been amply shown to exhibit structural and functional properties similar to those of larger, conventional muscle preparations (Bartoo *et al*., 1993; Linke *et al*., 1994, 1996b). By measuring both myofibrillar passive tension and the extension behavior of individual I-band titin segments during stretch, we could deduce the particular titin region responsible for sarcomere elasticity.

Interpretation of the results of immunofluorescence studies must consider the molecular architecture of I-band titin (Labeit & Kolmerer, 1995). Muscle tissue-specific length variations exist for both the tandem Ig domain and the PEVK region and result from alternative splicing pathways: apart from the short N2-titin segment, the elastic portion of human soleus I-band titin contains 90 tandem Ig repeats and a 2174-residue PEVK titin, whereas human cardiac I-band titin comprises 37 tandem Ig repeats and a 163-residue PEVK region for the N2-B-specific splice pathway (Labeit & Kolmerer, 1995; cf. also Figure 1). In human and rabbit psoas muscle, the tandem Ig and the PEVK region both exist in intermediate length versions, with, for example, rabbit psoas expressing 70 tandem Ig repeats and ~1400 residues of PEVK titin (unpublished results). The extension capacity of each region in a given muscle type can be estimated from our results, since it is known that (1) the N1-N2-titin segment consists solely of Ig repeats (Labeit & Kolmerer, 1995); (2) the N2-titin-A/I-junction region comprises both Ig repeats and the PEVK element and also includes an ~50 nm-long inextensible segment near the A/I-junction (Trombitas & Pollack, 1993); and (3) the Ig domains on either side of the N2-titin segment have similar stability and, probably, extensibility (Politou *et al*., 1996). Although in the latter study, only a few I-band Ig titin domains were selected for stability measurements, sequence alignment of the tandem Ig domains on either side of the N2-titin segment clearly defines them as a specific subgroup within the titin Ig family (Improta *et al*., 1996), so that the structurally studied domains appear to be representative of the entire tandem Ig domain family.

The pattern of translational movement of the antibodies indicates that in skeletal myofibrils, the N1-N2-titin segment (Ig domains) lengthens predominantly below SLs of 2.8 (soleus) or 2.6 (psoas) μm, but only little above these SLs (Figure 3A and B). Furthermore, with an individual, folded, Ig module ~4 nm in size (Whiting *et al*., 1989), the total, combined length of the Ig domains in a straightened, but not unfolded, state should be 360 nm per half-sarcomere in soleus, 280 nm in psoas, and 150 nm in cardiac muscle, respectively (as follows from the previous section). Considering that in addition, ~150 nm inextensible I-band domains exist per half-sarcomere in all three muscle types (Trombitas & Pollack, 1993; Trombitas *et al*., 1995), that A-bands are ~1.6 μm long, and that the (not or little extended) PEVK segment also

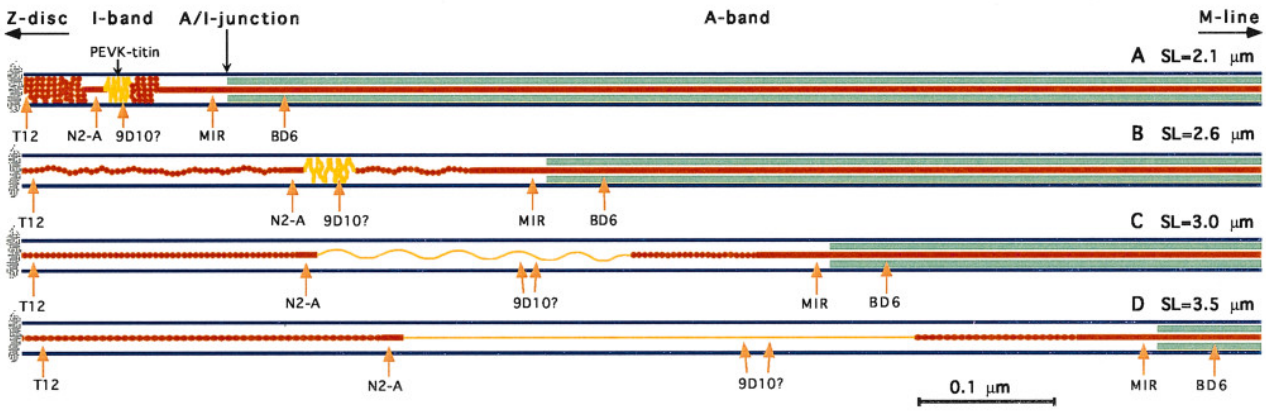

Figure 6. Model of titin extension with sarcomere stretch. Shown is a major portion of the half-sarcomere, including the I-band portion, which contains the elastic titin segment, at four different stages: A, slack SL; B, small stretch; C, moderate stretch; and D, extreme stretch. Color codes: blue, actin; green, myosin; yellow, PEVK titin; red, non-PEVK titin, with the filled circles representing the I-band Ig domains. T12, N2-A, MIR, BD6 = known binding sites of titin antibodies. 9D10? = possible epitope position of the 9D10 antibody; the arrow doublets in C and D indicate that the epitope widened at longer SLs. This model of titin arrangement reflects the situation in psoas muscle. For further explanation, see the text. Additional information on the proposed model of titin extension can be obtained from the world wide web from http://www.embl-heidelberg.de/ExternalInfo/Titin/.

adds somewhat to the length of I-band titin, we would calculate the SLs, at which I-band Ig domains are fully straightened (but still folded), to be 2.7 to 2.8, 2.5 to 2.6, and 2.2 to 2.3 µm, for soleus, psoas, and cardiac myofibrils, respectively. Remarkably, at least in the skeletal muscle specimens, these SLs correlate well with the SLs up to which we observed mainly lengthening of the Ig domain region. Such lengthening thus appears to be brought about by Ig domain straightening, and not by unfolding. In cardiac myofibrils, on the other hand, we found a continuous extension of the N1-N2-titin region over the entire SL range investigated (Figure 3C). Since we estimated the cardiac Ig repeats to be fully straightened at SLs of 2.2 to 2.3 µm, it follows that above these SLs, Ig domains should become unfolded.

In contrast, the N2-titin-A/I-junction region (Ig repeats + PEVK) was extensible over the entire SL range in all three muscle types. Clearly, in soleus and psoas myofibrils it must be mostly the PEVK element that represents the extensible titin domain at SLs greater than 2.8 and 2.6 µm, respectively. In cardiac sarcomeres, the short length of the PEVK region (Labeit & Kolmerer, 1995) appears to contribute only little to titin extensibility. Support for these conclusions also comes from the mobility pattern of the 9D10 antibody epitope. Figure 4 suggests that 9D10 binds C-terminally from the N2-titin segment, in a region where the PEVK titin sequence is expected. With small to extreme stretch, the 9D10 epitope moves away not only from the Z-disc, but also from the A/I-junction, which makes it unlikely that the antibody binds C-terminally within the constitutive I-band Ig region (cf. Figure 1). Rather, it is reasonable to assume, in combination with the other antibody mobility data, that 9D10 indeed binds within the PEVK segment. Therefore, we tentatively suggest that the slope differences between the N2-A titin and the 9D10 spacing curves (Figure 4) are a measure for PEVK domain extension.

These data combined with the results of passive tension measurements demonstrate that in skeletal myofibrils, a measurable passive force increase is not correlated with lengthening of the Ig domain region but rather with extension of the PEVK element (Figures 3A and B, 4A and B, 5A and B). Only in extremely stretched sarcomeres might Ig domain unfolding contribute to passive tension. In cardiac myofibrils, the short PEVK region could also support passive tension, but only over a very limited SL range, which might explain the onset of a steep passive tension rise shortly above ~2.2 µm SL (Figure 5C). After the PEVK extensibility has been exhausted, passive tension might be determined mainly by unfolding of Ig domains. However, since the physiological range of cardiac SLs ends near 2.4 µm (Allen & Kentish, 1985; Rodriguez *et al*., 1992), considerable Ig domain unfolding is unlikely to occur *in vivo*. In conclusion, it appears that the PEVK region of titin is the principal component responsible for myofibrillar passive tension and elasticity.

To sum up, the following scenario can be envisioned to explain the passive force response of titin filaments to stretch (Figure 6). At slack SL, I-band titin is flaccid, with the Ig domains and the PEVK element in the folded state (A). During a small stretch, Ig domains straighten, but the PEVK region remains almost completely folded, resulting in no measurable passive tension (B). With a moderate stretch, Ig domains barely extend further, whereas the PEVK region unravels, which results in a steady passive tension increase (C). At extremely stretched SLs (toward the high end of the physiological SL range), the PEVK element is maximally unravelled and the Ig domains become

highly strained; passive tension now reaches a maximum before previously bound A-band titin is released into the I-band (D). Along this line of reasoning, we suggest that the expression of different length versions of tandem Ig domain segments in various muscle types (Labeit & Kolmerer, 1995) may be important for setting the physiological slack SL, whereas differential splicing of PEVK sequences controls tissue-specificity of passive stiffness.

At present, the molecular basis of PEVK domain elasticity is obscure. It is clear from this study that the PEVK region is able to lengthen maximally by approximately 600 to 700 nm per half-sarcomere in soleus myofibrils (cf. Figures 3A and 4A). Since the soleus PEVK sequence comprises ~2200 residues, it follows that each residue, in the stretched state, must span ~0.3 nm, about two thirds of the possible maximum of 0.42 nm for extended polypeptide chains. The conformational changes that may occur within the PEVK sequence to allow such remarkable extensibility are still unclear. We have calculated the force required for maximum extension of one titin molecule's PEVK region, based on the measured passive tension magnitude of single skeletal myofibrils at strain limit SL (cf. Linke *et al*., 1994). With the assumption that a myofibril approximately 1 μm in diameter consists of ~1000 to 2000 titin molecules in parallel (as follows from the number of three to six titin strands per thick filament and half-sarcomere; Maruyama, 1994), we inferred this maximum force to be of the order of a few tens of pN. Furthermore, when no forces are applied and I-band titin is retracted, the PEVK element appears to adopt a compact conformation. Electron micrographs of native, isolated titin molecules have failed to reveal the presence of a PEVK segment (Nave *et al*., 1989), presumably because they show this segment in a state in which it is apparently folded into a cylindrical region of similar diameter to that of the flanking Ig domains. From these observations, and also from the fact that the PEVK sequences in different species show a high degree of conservation among vertebrates (C. Witt, unpublished results), we conclude that the PEVK titin, in the retracted state, does not simply collapse but may adopt a defined fold. The nature of such a fold, however, is still unknown. Clearly, further studies are needed to characterize the mechanism of PEVK domain folding and unravelling, and to fully understand how this region can constitute a highly extensible spring that accounts for the elasticity of vertebrate striated muscle.

Materials and Methods

Myofibril preparation

Single myofibrils were prepared from both fresh and glycerinated, cardiac and skeletal, muscle tissue according to the method of Knight & Trinick (1982). Briefly, thin strips from rat (sometimes also rabbit) right ventricle, psoas, and soleus muscle were dissected and either stored in rigor/glycerol (1:1, v/v) solution or, for immediate use, skinned in rigor solution containing 1% (v/v) Triton X-100. To obtain single myofibrils, the skinned strips were minced and homogenized in rigor (blender, Ultra-Turrax) at 4°C. From the suspension of myofibrils, a drop was placed in the specimen chamber, and myofibrils were allowed to settle. Then, one single myofibril (sometimes also a doublet) was picked up by two glass microneedles, which could be controlled by hydraulic micromanipulators (Narishige, Japan). Solutions used had an ionic strength of 200 mM (pH 7.1) and contained 20 μg/ml protease inhibitor, leupeptin (cf. Linke *et al*., 1994). Experiments were performed at room temperature.

Antibodies

Polyclonal antibodies N2-A and N2-B were raised to expressed titin sequences from the N2-titin segment. Those antibodies are specific to the splice pathways N2-A and N2-B, respectively. For N2-A, base-pairs 15607 to 15957 of the human skeletal titin sequence (EMBL data library X90569), for N2-B, base-pairs 10354 to 11115 of the human cardiac titin sequence, (EMBL data library X90568), were isolated by PCR (Saiki *et al*., 1985), subcloned into His-tagged pET vectors, and expressed in *E. coli* and purified (Studier *et al*., 1990; LeGrice & Grueniger-Leitch, 1990). Polyclonal antibodies to the expressed antigens were raised in rabbits according to standard protocols.

Antibodies T12, BD6, MIR and 9D10 were obtained from other sources: monoclonal IgG antibodies T12 and BD6 were kindly provided by D. O. Fürst and J. Trinick, respectively (cf. Fürst *et al*., 1988; Whiting *et al*., 1989), the monoclonal IgM, 9D10, by M. L. Greaser (Wang & Greaser, 1985), and the MIR sera by J. A. Aarli (Aarli *et al*., 1990). 9D10 was also obtained from the Hybridoma Bank, University of Iowa, Iowa City, IA.

As secondary antibodies, we used rhodamine-conjugated anti-rabbit or anti-mouse IgG (whole molecule, SIGMA, No. T-5269 and T-5393, respectively). Although the 9D10 antibody is an IgM, we obtained good results using anti-mouse IgG as a secondary antibody. For the MIR antibody, we also used anti-human IgG, whole molecule, SIGMA, No. T-5903.

Immunofluorescence microscopy

Fluorescence measurements were performed under an inverted microscope (Zeiss Axiovert, epifluorescence modus, 100× oil immersion objective). The myofibril image was recorded using a high-resolution CCD video camera (FK440, Völker, Maintal, Germany), video recorder (Panasonic NV-SD45), and/or frame grabber board (Vision-EZ, Data Translation). With image processing techniques (Global Lab Image, Data Translation), the centroid coordinate of a fluorescent antibody epitope could be detected with a precision of ±40 to ±80 nm. At a given SL, we usually recorded at least two fluorescence images, which were then superimposed to increase resolution. Two alternative experimental protocols were used. In the first, a relaxed myofibril was set to slack SL, was labelled with one of the primary antibodies and after washout, was secondary labelled with rhodamine-conjugated IgG. The primary and secondary antibodies were normally used in dilutions of 1:50 and 1:80 (in relaxing solution), respectively; exposure time to myofibrils was 10 to 30 minutes. After labelling, the myofibril was stretched slowly (about 10% of its initial length per minute) to a series of SLs, and the translational

movement of the antibody epitopes was recorded. In a second experimental protocol, the myofibril was stretched first to a desired SL above slack and was then labelled with the antibody and fluorophore. Both measurement protocols gave similar results. As a control, we labelled myofibrils with the secondary antibody only, and found no fluorescence. Additional information on the mechanics of fluorescently labelled single myofibrils is available from http://www.embl-heidelberg.de/ExternalInfo/Titin/.

Force measurements

The setup used for passive tension recordings is essentially similar to that described previously (Bartoo *et al*., 1993; Linke *et al*., 1993). It is centered around a Zeiss Axiovert microscope equipped with phase-contrast optics. The specimen is suspended between the two glass needle tips (glue, Dow Corning 3145 RTV), one attached to a piezoelectric micromotor, the other to a home-built force transducer. The transducer, which operates on the basis of optical fiber beams, has a sensitivity of ~ 5 nN, at a resonant frequency of 500 Hz in water (Fearn *et al*., 1993). The myofibril image can be recorded with either a 512-element linear photodiode array (Reticon electronics) or the CCD video camera and video recorder. Data collection is done with a PC and National Instruments data acquisition board (including Labview software).

Mechanics protocols were performed as follows (cf. Linke *et al*., 1994): A relaxed myofibril was held at slack length and was then stretched in stages to a series of desired SLs. Stretch duration was five to ten seconds. At the stretched lengths, we generally observed a stress-relaxation-based force decay, which increased with stretch to larger SLs. Before being stretched to the next experimental length, the specimen was held at constant SL for two to three minutes, so that force could decay to a steady-state level. Following stretch to a desired maximum length, a progressive release protocol was performed, so that finally the specimen returned to slack SL. Force was continuously measured at intervals of 5 to 20 ms.

To obtain force per myofibril cross-sectional area, we recorded myofibril width at slack SL and measured it by analyzing the intensity profile perpendicular to the myofibril axis, in the myofibril's center. Image-processing software was the same as that mentioned above. From the profile plot, pixel positions at half-maximum peak height were taken to define the two edges of the myofibril (error, approximately ± 160 nm). Cross-sectional area was calculated by assuming a circular shape of the myofibril.

As a control to test the effect of antibody binding on titin-filament compliance, we measured passive force before and after labelling with both the primary and secondary antibodies. Primary antibody labelling did not measurably affect myofibril stiffness, whereas additional staining with the secondary antibodies somewhat increased stiffness. Therefore, passive length-tension curves were generally measured in non-labelled specimens. As for the immunofluorescence measurements, an effect of myofibril stiffening on the titin epitope extension behavior could be excluded, since both measurement protocols mentioned above (cf. Immunofluorescence microscopy) gave similar results.

Acknowledgements

We thank J. Trinick, D. O. Fürst, M. L. Greaser, and J. A. Aarli for kindly supplying the BD6, T12 and 9D10 antibodies, and the MIR sera, respectively. We also thank C. Witt for communicating unpublished results, A. Pastore, T. Gibson and M. Saraste for helpful discussions, and R. Wojciechowski for expert technical assistance. We gratefully acknowledge the financial support of the Deutsche Forschungsgemeinschaft, the Universitäts-Frauenklinik Mannheim der Klinischen Fakultät Mannheim-Heidelberg, and the EU.

References

Aarli, J. A., Stefansson, K., Marton, L. S. G. & Wollmann, R. L. (1990). Patients with myasthenia gravis and thymoma have in their sera IgG autoantibodies against titin. *Clin. Exp. Immunol.* **82**, 284–288.

Allen, D. G. & Kentish, J. C. (1985). The celluar basis of the length-tension relation in cardiac muscle. *J. Mol. Cell. Cardiol.* **17**, 821–840.

Bartoo, M. L., Popov, V. I., Fearn, L. A. & Pollack, G. H. (1993). Active tension generation in isolated skeletal myofibrils. *J. Muscle Res. Cell Motil.* **14**, 498–510.

Erickson, H. P. (1994). Reversible unfolding of fibronectin type III and immunoglobulin domains provides the structural basis for stretch and elasticity of titin and fibronectin. *Proc. Natl Acad. Sci. USA*, **91**, 10114–10118.

Fearn, L. A., Bartoo, M. L., Myers, J. A. & Pollack, G. H. (1993). An optical fiber transducer for single myofibril force measurement. *IEEE Trans. Biomed. Eng.* **40**, 1127–1132.

Fürst, D. O., Osborn, M., Nave, R. & Weber, K. (1988). The organization of titin filaments in the half-sarcomere revealed by monoclonal antibodies in immunoelectron microscopy: a map of ten nonrepetitive epitopes starting at the Z-line extends close to the M-line. *J. Cell Biol.* **106**, 1563–1572.

Funatsu, T., Kono, E., Higuchi, H., Kimura, S., Ishiwata, S., Yoshioka, T., Maruyama, K. & Tsukita, S. (1993). Elastic filaments *in situ* in cardiac muscle: deep-etch replica analysis in combination with selective removal of actin and myosin filaments. *J. Cell Biol.* **120**, 711–724.

Gautel, M., Lakay, A., Barlow, D. P., Holmes, Z., Scales, S., Leonard, K., Labeit, S., Mygland, A., Gilhus, N. E. & Aarli, J. A. (1993). Titin antibodies in myasthenia gravis: identification of a major immunogenic region of titin. *Neurology*, **43**, 1581–1585.

Granzier, H. L. & Wang, K. (1993). Passive tension and stiffness of vertebrate skeletal and insect flight muscles: the contribution of weak cross-bridges and elastic filaments. *Biophys. J.* **65**, 2141–2159.

Granzier, H. L. & Irving, T. C. (1995). Passive tension in cardiac muscle: contribution of collagen, titin, microtubules and intermediate filaments. *Biophys. J.* **68**, 1027–1044.

Granzier, H., Helmes, M. & Trombitas, K. (1996). Nonuniform elasticity of titin in cardiac myocytes: a study using immunoelectron microscopy and cellular mechanics. *Biophys. J.* **70**, 430–442.

Holden, H. M., Ito, M., Hartshorne, D. J. & Rayment, I. (1992). X-ray structure determination of telokin, the C-terminal domain of myosin light chain kinase, at 2.8 Å resolution. *J. Mol. Biol.* **227**, 840–851.

Horowits, R. (1992). Passive force generation and titin isoforms in mammalian skeletal muscle. *Biophys. J.* **61**, 392–398.

Horowits, R., Kempner, E. S., Bisher, M. E. & Podolski, R. J. (1986). A physiological role for titin and nebulin in skeletal muscle. *Nature,* **323**, 160–164.

Improta, S., Politou, A. S. & Pastore, A. (1996). Immunoglobulin-like modules from titin I-band: extensible components of muscle elasticity. *Structure,* **4**, 323–337.

Itoh, Y., Suzuki, T., Kimura, S., Ohashi, K., Higuchi, H., Sawada, H., Shimizu, T., Shibata, M. & Maruyama, K. (1988). Extensible and less-extensible domains of connectin filaments in stretched vertebrate skeletal muscle as detected by immunofluorescence and immunoelectron microscopy using monoclonal antibodies. *J. Biochem. (Tokyo),* **104**, 504–508.

Knight, P. J. & Trinick, J. A. (1982). Preparation of myofibrils. *Methods Enzymol.* **85**, 9–12.

Labeit, S. & Kolmerer, B. (1995). Titins, giant proteins in charge of muscle ultrastructure and elasticity. *Science*, **270**, 293–296.

Labeit, S., Barlow, D., Gautel, M., Gibson, T., Holt, J., Hsieh, C.-L., Francke, U., Leonard, K., Wardale, J., Whiting, A. & Trinick, J. (1990). A regular pattern of two types of 100-residue motif in the sequence of titin. *Nature*, **345**, 273–276.

Leahy, D. J., Hendrickson, W. A., Aukhil, I. & Erickson, H. P. (1992). Structure of a fibronectin type III domain from tenascin phased by MAD analysis of the selenomethionyl protein. *Science,* **258**, 987–990.

LeGrice, S. F. J. & Grueninger-Leitch, F. (1990). Rapid purification of homodimer and heterodimer HIV-1 reverse transcriptase by metal chelate affinity chromatography. *Eur. J. Biochem.* **187**, 307–314.

Linke, W. A., Bartoo, M. L. & Pollack, G. H. (1993). Spontaneous sarcomeric oscillations at intermediate activation levels in single isolated myofibrils. *Circ. Res.* **73**, 724–734.

Linke, W. A., Popov, V. I. & Pollack, G. H. (1994). Passive and active tension in single cardiac myofibrils. *Biophys. J.* **67**, 782–792.

Linke, W. A., Ivemeyer, M., Rüegg, J. C. & Labeit, S. (1996a). Evidence for a highly extensible titin domain that accounts for vertebrate muscle elasticity. *Pflügers Arch.* **431 (6**, **suppl**.), R39.

Linke, W. A., Bartoo, M. L., Ivemeyer, M. & Pollack, G. H. (1996b). Limits of titin extension in single cardiac myofibrils. *J. Muscle Res. Cell Motil*. In the press.

Magid, A. & Law, D. J. (1985). Myofibrils bear most of the resting tension in frog skeletal muscle. *Science*, **230**, 1280-1282.

Maruyama, K. (1994). Connectin, an elastic protein of striated muscle. *Biophys. Chem.* **50**, 73–85.

Maruyama, K., Matsubara, S., Natori, R., Nonomura, Y., Kimura, S., Ohashi, K., Murakami, F., Handa, S. & Eguchi, G. (1977). Connectin, an elastic protein of muscle: characterization and function. *J. Biochem. (Tokyo),* **82**, 317–337.

Nave, R., Fürst, D. O. & Weber, K. (1989). Visualization of the polarity of isolated titin molecules: a single globular head on a long thin rod as the M band anchoring domain? *J. Cell. Biol.* **109**, 2177–2187.

Pfuhl, M. & Pastore, A. (1995). Tertiary structure of an immunoglobulin-like domain from the giant muscle protein titin: a new member of the I set. *Structure,* **3**, 391–401.

Politou, A. S., Thomas, D. J. & Pastore, A. (1995). The folding and stability of titin immunoglobulin-like modules, with implications for the mechanism of elasticity. *Biophys. J.* **69**, 2601–2610.

Politou, A. S., Gautel, M., Improta, S., Vangelista, L. & Pastore, A. (1996). The elastic I-band region of titin is assembled in a ''modular'' fashion by weakly interacting Ig-like domains. *J. Mol. Biol.* **255**, 604–616.

Rodriguez, E. K., Hunter, W. C., Royce, M. J., Leppo, M. K., Doulas, A. S. & Weisman, H. F. (1992). A method to reconstruct myocardial sarcomere lengths and orientations at transmural sites in beating canine hearts. *Am. J. Physiol.* **263**, H293–H306.

Saiki, R. K., Scharf, S., Faloona, F., Mullis, K. B., Horn, G. T., Ehrlich, H. A. & Arnheim, N. (1985). Enzymatic amplification of beta-globin genomic sequences and restriction site analysis for diagnosis of sickle cell anemia. *Science,* **230**, 1350–1354.

Salviati, G., Betto, R., Ceoldo, S. & Pierobon-Bormioli, S. (1990). Morphological and functional characterization of the endosarcomeric elastic filament. *Am. J. Physiol.* **259**, C144–C149.

Sebestyen, M. G., Wolff, J. A. & Greaser, M. L. (1995). Characterization of a 5.4 kb cDNA fragment from the Z-line region of a rabbit cardiac titin reveals phosphorylation sites for proline-directed kinases. *J. Cell Sci.* **108**, 3029–3037.

Soteriou, A., Clarke, A., Martin, S. & Trinick, J. (1993). Titin folding energy and elasticity. *Proc. Roy. Soc. ser. B,* **254**, 83–86.

Studier, F. W., Rosenberg, A. H., Dunn, J. J. & Dubendorff, J. W. (1990). Use of T7 RNS polymerase to direct expression of cloned genes. *Methods Enzymol.* **185**, 60–89.

Trinick, J. (1994). Titin and nebulin: protein rulers in muscle? *Trends Biochem. Sci.* **19**, 405–409.

Trombitas, K. & Pollack, G. H. (1993). Elastic properties of the titin filament in the Z-line region of vertebrate striated muscle. *J. Muscle Res. Cell Motil.* **14**, 416–422.

Trombitas, K., Baatsen, P. H. W. W., Kellermayer, M. S. Z. & Pollack, G. H. (1991). Nature and origin of gap filaments in striated muscle. *J. Cell Sci.* **100**, 809–814.

Trombitas, K., Jin, J.-P. & Granzier, H. (1995). The mechanically active domain of titin in cardiac muscle. *Circ. Res.* **77**, 856–861.

Wang, K., McClure, J. & Tu, A. (1979). Titin: Major myofibrillar component of striated muscle. *Proc. Natl Acad. Sci. USA*, **76**, 3698–3702.

Wang, K., McCarter, R., Wright, J., Beverly, J. & Ramirez-Mitchell, R. (1991). Regulation of skeletal muscle stiffness and elasticity by titin isoforms: a test of the segmental extension model of resting tension. *Proc. Natl Acad. Sci. USA*, **88**, 7101–7105.

Wang, K., McCarter, R., Wright, J., Beverly, J. & Ramirez-Mitchell, R. (1993). Viscoelasticity of the sarcomere matrix of skeletal muscles; the titin-myosin composite filament is a dual-stage molecular spring. *Biophys. J.* **64**, 1161–1177.

Wang, S.-M. & Greaser, M. L. (1985). Immunocytochemical studies using a monoclonal antibody to bovine cardiac titin on intact and extracted myofibrils. *J. Muscle Res. Cell Motil.* **6**, 293–312.

Whiting, A., Wardale, J. & Trinick, J. (1989). Does titin regulate the length of muscle thick filaments? *J. Mol. Biol.* **205**, 163–169.

Edited by J. Karn

(Received 26 March 1996; received in revised form 20 May 1996; accepted 22 May 1996)